The EMBO Journal Vol. 21 No. 15 pp. 4012–4025, 2002

The Rho-GAP Bem2p plays a GAP-independent role in the morphogenesis checkpoint

Aron R.Marquitz, Jacob C.Harrison, Indrani Bose[1], Trevin R.Zyla, John N.McMillan and Daniel J.Lew[2]

Department of Pharmacology and Cancer Biology, Duke University Medical Center, Durham, NC 27710, USA

[1]Present address: Department of Molecular Microbiology, Washington University School of Medicine, St Louis, MO 63110, USA

[2]Corresponding author
e-mail: daniel.lew@duke.edu

The *Saccharomyces cerevisiae* morphogenesis checkpoint delays mitosis in response to insults that impair actin organization and/or bud formation. The delay is due to accumulation of the inhibitory kinase Swe1p, which phosphorylates the cyclin-dependent kinase Cdc28p. Having screened through a panel of yeast mutants with defects in cell morphogenesis, we report here that the polarity establishment protein Bem2p is required for the checkpoint response. Bem2p is a Rho-GTPase activating protein (GAP) previously shown to act on Rho1p, and we now show that it also acts on Cdc42p, the GTPase primarily responsible for establishment of cell polarity in yeast. Whereas the morphogenesis role of Bem2p required GAP activity, the checkpoint role of Bem2p did not. Instead, this function required an N-terminal Bem2p domain. Thus, this single protein has a GAP-dependent role in promoting cell polarity and a GAP-independent role in responding to defects in cell polarity by enacting the checkpoint. Surprisingly, Swe1p accumulation occurred normally in *bem2* cells, but they were nevertheless unable to promote Cdc28p phosphorylation. Therefore, Bem2p defines a novel pathway in the morphogenesis checkpoint.

Keywords: Bem2p/cell cycle/checkpoint/Rho-GAP/*Saccharomyces cerevisiae*

Introduction

In all eukaryotic cells, the G_2/M transition is controlled by the cyclin-dependent kinase Cdc2 (Cdc28p in *Saccharomyces cerevisiae*), whose activity is in turn tightly regulated by the countervailing activities of inhibitory Wee1-family kinases (Swe1p in *S.cerevisiae*) and stimulatory Cdc25-family phosphatases (Mih1p in *S.cerevisiae*) (reviewed by Coleman and Dunphy, 1994; O'Farrell, 2001). In many cells, the Wee1/Cdc25 balance is tilted firmly in favor of Wee1 during G_2, resulting in the accumulation of phosphorylated and inhibited Cdc2 complexes. An ill-defined initiating event then tilts the balance in favor of Cdc25, promoting dephosphorylation and activation of Cdc2, with consequent entry into mitosis. Checkpoint controls responding to DNA damage or incomplete DNA replication delay entry into mitosis by maintaining the G_2 supremacy of the inhibitory Wee1-family kinases.

A rather different situation exists in the budding yeast *S.cerevisiae*, where the mitotic Cdc28p complexes do not appear to be significantly restrained by inhibitory phosphorylation (Amon *et al*., 1992; Sorger and Murray, 1992). In this organism, the Swe1p/Mih1p balance is tilted firmly in favor of the phosphatase Mih1p, for at least two reasons. First, Swe1p is only synthesized during late G_1 phase (Sia *et al*., 1996) and is largely degraded by the time of mitosis (Sia *et al*., 1998). Secondly, even when Swe1p is stabilized by mutation of Swe1p degradation factors, Mih1p is sufficiently active to overcome Swe1p-mediated Cdc28p inhibition and cells experience only a modest G_2 delay (Ma *et al*., 1996; McMillan *et al*., 1999). In combination, the degradation of Swe1p and the activity of Mih1p ensure that very little Cdc28p inhibition occurs in the unperturbed cell cycle.

In *S.cerevisiae*, the DNA damage and DNA replication checkpoint controls do not block Cdc28p activation (Sorger and Murray, 1992; Stueland *et al*., 1993), but rather act later in the cell cycle to inhibit the metaphase–anaphase transition (Yamamoto *et al*., 1996). In contrast, a 'morphogenesis checkpoint' acts to inhibit mitotic Cdc28p complexes by tilting the Swe1p/Mih1p balance in favor of Swe1p. This checkpoint pathway responds to a variety of environmental and experimental insults that impair bud formation (e.g. changes in temperature or osmolarity that depolarize actin, or drugs that depolymerize actin) (Lew and Reed, 1995; McMillan *et al*., 1998). The G_2 delay provided by the checkpoint allows cells to recover from the insult and complete bud formation prior to undergoing nuclear division. To tilt the Swe1p/Mih1p balance in favor of Swe1p, the morphogenesis checkpoint halts the degradation of Swe1p (Sia *et al*., 1998) and activates a kinase cascade culminating in the MAPK Mpk1p/Slt2p, which is thought to downregulate Mih1p (Harrison *et al*., 2001).

We are particularly interested in understanding how the morphogenesis checkpoint detects the perturbations that impair bud formation. Studies on the DNA replication checkpoint revealed that mutations affecting components of the replication fork could render cells unable to delay the cell cycle in response to arrest of DNA replication, suggesting that the source for the checkpoint signal was the stalled replication fork itself (Araki *et al*., 1995; Navas *et al*., 1995; Sugimoto *et al*., 1996). By analogy, we reasoned that the morphogenesis checkpoint may monitor some 'bud formation complex', so that mutations in components of that complex might render the checkpoint ineffective.

Studies of yeast morphogenesis have supported a hierarchical model for bud formation in which 'bud-site

selection' proteins act to localize the activity of 'polarity establishment' proteins, which in turn polarize the actin cytoskeleton and hence the secretory pathway to form a bud (reviewed by Pringle *et al*., 1995; Pruyne and Bretscher, 2000a,b). We tested mutant strains defective in a variety of proteins involved at each of these steps to determine whether any would be defective for the morphogenesis checkpoint. Here we report that one of these mutants, lacking the polarity establishment protein Bem2p, was uniquely defective in this regard.

Bem2p is a 246 kDa protein with a 160 amino acid Rho-GAP domain at its C-terminus (Peterson *et al*., 1994). Although the GAP activity of Bem2p was important for its role in polarity establishment, this activity was dispensable for its checkpoint function. Surprisingly, *bem2*Δ mutants were fully competent to stabilize Swe1p and to activate Mpk1p in response to actin depolymerization, but they nevertheless failed to inhibit Cdc28p and arrest the cell cycle. These studies therefore indicate the existence of a novel branch of the morphogenesis checkpoint that involves a non-enzmatyic function of the Rho-GAP Bem2p.

Results

A specific requirement for Bem2p in the morphogenesis checkpoint

Reasoning that proteins functioning in the process of bud formation might be ideally placed to monitor the progress of bud formation, we examined checkpoint function in strains containing mutations in various genes known to be involved in that process. To assess checkpoint function, stationary phase cells were inoculated into fresh medium containing latrunculin-B (Lat-B), which partially depolymerizes actin and prevents bud formation. Wild-type cells arrest cell cycle progression in G_2 under these conditions, whereas cells defective for checkpoint function (e.g. *swe1*Δ mutants) continue with the cell cycle and become binucleate (McMillan *et al*., 1998). Thus, DNA staining provides a rapid and simple assay to test whether or not mutant cells have an intact checkpoint. We found that mutants in genes encoding known bud site selection components or actin cytoskeleton components all arrested the cell cycle upon actin depolymerization (Table I). Similar results were obtained in tests of mutant strains carrying a series of alanine scanning mutations in the *ACT1* gene (encoding the sole yeast actin), as well as mutations in most polarity establishment genes (Table I). The only mutants, other than *swe1*Δ, which displayed significant numbers of binucleate cells following Lat-B treatment were *bem1*Δ and *bem2*Δ (Figure 1A).

The *BEM1* and *BEM2* genes (bud emergence) were first identified in a screen for mutants that were synthetic lethal in combination with loss of *MSB1* (multicopy suppressor of budding) (Bender and Pringle, 1991), which was itself identified as a suppressor of both *cdc24* and *cdc42* mutants (Bender and Pringle, 1989). Subsequent studies demonstrated numerous genetic interactions between these mutations and others involved in bud site selection, polarity establishment and the actin cytoskeleton (Chant *et al*., 1991; Wang and Bretscher, 1995; Bender *et al*., 1996; Chen *et al*., 1996; Oehlen and Cross, 1998; Tong *et al*., 2001). *bem1*Δ and *bem2*Δ are among the most

Table I. Yeast strains tested for morphogenesis checkpoint

Genotype	Description	Binucleates in Lat-B
Bud site selection genes		
*rsr1*Δ	Ras-like regulator of bud site selection	–
*bud2*Δ	GAP for Rsr1p	–
*bud5*Δ	GEF for Rsr1p	–
*rsr1*Δ *bud8*Δ	Bud8p: landmark for bipolar budding	–
*spa2*Δ	Required for bipolar budding and shmoo formation	–
*bni1*Δ	Formin homolog	–
*aip3*Δ*2*	= Bud6p required for bipolar budding	–
Polarity establishment genes		
cdc24-1[a]	GEF for Cdc42p	–
*bem1*Δ	Scaffold for polarity establishment proteins	+++
*bem2*Δ	Rho GAP	+++
*cla4*Δ	PAK kinase, Cdc42p effector	–
*ste20*Δ	PAK kinase, Cdc42p effector	–
*gic1*Δ *gic2*Δ	Cdc42p effectors	–
*msb1*Δ	Unknown function	–
*msb3*Δ *msb4*Δ	Rab GAPs	–
*rho2*Δ	Rho GTPase	–
*rho4*Δ	Rho GTPase	–
Actin and actin-associated proteins		
act1-101	Actin	–
act1-102	Actin	–
act1-105	Actin	–
act1-108	Actin	–
act1-111	Actin	+/–[b]
act1-115	Actin	–
act1-116	Actin	–
act1-119	Actin	–
act1-120	Actin	+/–[b]
act1-121	Actin	–
act1-122	Actin	–
act1-123	Actin	–
act1-124	Actin	–
act1-129	Actin	–
act1-132	Actin	–
act1-133	Actin	–
act1-135	Actin	–
act1-136	Actin	–
*cap2*Δ	Actin filament capping protein	–
*tpm1*Δ	Tropomyosin, actin filament binding	–
*sac6*Δ	Fimbrin, actin filament bundling	–
cof1-4	Cofilin, actin filament severing	–
cof1-5	Cofilin, actin filament severing	–
cof1-22	Cofilin, actin filament severing	–
*abp1*Δ	Actin binding protein, cortical patch component	–
pfy1-111	Profilin, actin monomer binding	–
pfy1-112	Profilin, actin monomer binding	–
pfy1-116	Profilin, actin monomer binding	–
*myo1*Δ	Type II myosin, cytokinesis	–
myo2-66	Type V myosin, organelle and vesicle transport	–
*myo4*Δ	Type V myosin, mRNA localization	–
*myo3*Δ	Type I myosin, cortical patch component	–
*myo5*Δ	Type I myosin, cortical patch component	–
Septins		
cdc10-1[a]	Septin	–
cdc11-6[a]	Septin	–

[a]These strains were assayed at the restrictive temperature of 37°C.
[b]These two strains showed a smaller but reproducible accumulation of binucleated cells, but this phenotype was not recapitulated upon transfer of the *act1* mutations to strain BF264-15D.

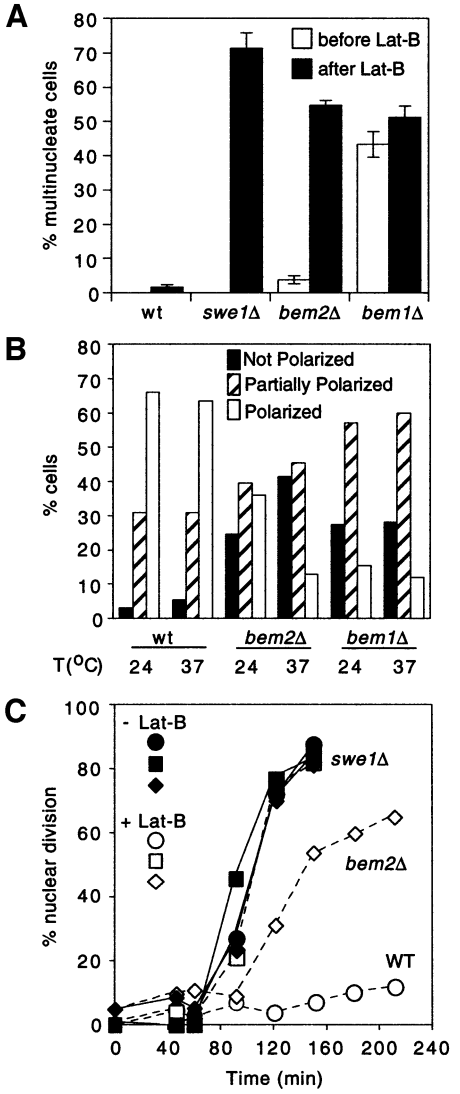

Fig. 1. Morphogenesis checkpoint in *bem2*Δ cells. (**A**) The indicated strains were grown to exponential phase in YEPD at 24°C and then resuspended in YEPD + 100 μM Lat-B and grown for 5 h. Cells were then fixed and stained with DAPI to visualize nuclei. Percentages of unbudded cells with multiple (>2) nuclei were scored for each strain before and after the growth in Lat-B. (**B**) The indicated strains were grown to exponential phase in YEPD at the indicated temperature, fixed and stained to visualize F-actin. Budded cells with an undivided nucleus were scored as polarized (all actin patches in bud), partially polarized (large majority of patches in bud), or not polarized (random distribution of actin patches). In the case of the *bem1*Δ mutant, a large proportion of the cells had >1 nucleus (A), and the multinucleate cells were uniformly worse in terms of actin polarity than the cells with a single nucleus. Our scoring therefore measured only the best polarized of the *bem1*Δ cells, and overall the polarity defect was more pronounced in *bem1*Δ than in *bem2*Δ mutants. (**C**) The indicated strains were synchronized in G_1 with α-factor and released into fresh YEPD at 24°C. After release (30 min), cells were resuspended in 100 μM Lat-B (+) or DMSO (–) as a vehicle control. At the indicated time points, cells were fixed and stained with DAPI to score nuclear division. Strains: DLY1 (WT), DLY4021 (*swe1*Δ), DLY4015 (*bem2*Δ) and JMY1011 (*bem1*Δ).

severely depolarized of all of the viable mutants that we tested, raising the possibility that the apparent checkpoint defect might be a consequence of the constitutively disorganized cytoskeleton exhibited by these mutants. However, further analysis showed that the basis for the observed accumulation of binucleate cells in these mutants was distinct. In particular, the *bem1*Δ cells, which displayed the most severe polarity defect (Figure 1A and B, see legend), managed to proliferate with a constitutively high proportion of multinucleate cells in the population even in the absence of Lat-B treatment. This proportion did not increase significantly in response to Lat-B (Figure 1A), suggesting that the checkpoint was intact in this mutant despite the severe constitutive depolarization. In contrast, the *bem2*Δ mutant appeared somewhat healthier and proliferated with many fewer multinucleate cells in the population, but showed a dramatic increase in the proportion of multinucleate cells following treatment with Lat-B (Figure 1A). To assess the behavior of this mutant in more detail, the kinetics of nuclear division were examined in synchronous cultures released from a pheromone-mediated G_1 arrest to traverse the cell cycle in the presence or absence of Lat-B. In this experiment, the *bem2*Δ cells treated with Lat-B displayed only a small (~1 h) delay in nuclear division compared with the untreated controls (Figure 1C). Wild-type cells arrested prior to nuclear division in the presence of Lat-B, whereas *swe1*Δ cells proceeded with nuclear division regardless of Lat-B (Figure 1C), as expected from previous work. We conclude that Bem2p, alone of all the bud formation proteins tested, is specifically required for the morphogenesis checkpoint to arrest the cell cycle in response to actin depolymerization.

GAP activity of Bem2p and the morphogenesis checkpoint

Bem2p is one of 11 proteins encoded in the yeast genome that contain a putative Rho-GAP domain. To assess which subset of these proteins might be important for checkpoint function, we assayed the effectiveness of the checkpoint in strains containing deletion alleles for each of these genes. Strikingly, only the *bem2*Δ strain had a significant checkpoint defect (Figure 2A), suggesting that the checkpoint role is restricted to Bem2p and not linked to general Rho-GAP activity.

To test whether the GAP activity of Bem2p was required for its function in the checkpoint, we first generated a C-terminal truncation of Bem2p lacking the GAP domain (residues 1959–2167). This *bem2*-Δ1959–2167 allele behaved as a *bem2*Δ null mutant both with regard to morphogenesis and with regard to checkpoint function (data not shown). Although this result is consistent with the hypothesis that the GAP domain is critical for all Bem2p functions, it is also possible that the truncation impairs the three-dimensional folding of Bem2p, indirectly inactivating some function(s) of the large non-catalytic domain. To address this possibility, we generated two single amino acid mutations in conserved residues that have been shown to be important for the activity of the mammalian p190 Rho-GAP (Figure 3A) (Li *et al.*, 1997). The crystal structure of several mammalian Rho-GAP domains has been solved (Musacchio *et al.*, 1996; Barrett *et al.*, 1997), revealing that Arg1283 participates directly in catalysis as part of the 'arginine finger', and that Lys1321 is an important contact point for Rho binding (Musacchio *et al.*, 1996; Barrett *et al.*, 1997). The R1283L and K1321A mutations therefore abolish GAP activity, without disturbing the overall folding of the

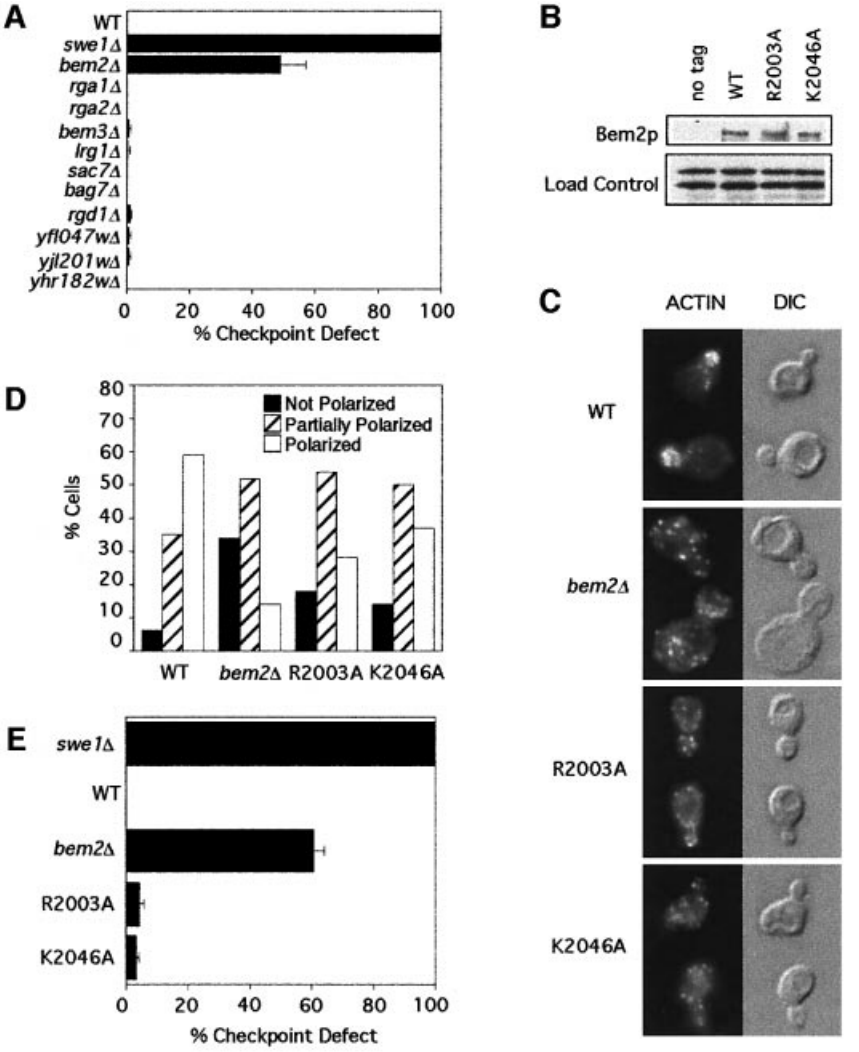

Fig. 2. Bem2p GAP activity and the morphogenesis checkpoint. (**A**) Homozygous diploid mutant strains of the indicated genotype were assayed for their ability to arrest the cell cycle when released from stationary phase into 100 μM Lat-B at 24°C. Percent checkpoint defect was calculated as the increase in binucleates due to Lat-B in the indicated strain as compared with the increase in the *swe1*Δ control strain, which was set to 100%. (**B**) The indicated strains were grown to exponential phase in YEPD at 30°C, pelleted and lysed. Lysates were separated by SDS–PAGE and immunoblotted with anti-myc antibody. (**C**) The indicated strains were grown to exponential phase in YEPD at 30°C, fixed and stained to visualize F-actin. (**D**) Actin polarity of samples was scored as in Figure 1B. Note that expression of wild-type BEM2 with a myc tag (WT) causes a slight polarity defect. (**E**) The indicated strains were assayed for checkpoint function as in (A). Strains: DLY1 (no tag), DLY4021 (*swe1*Δ), DLY4015 (*bem2*Δ), DLY4860 (WT), DLY5041 (R2003A) and DLY4862 (K2046A).

GAP domain. We made the analogous R2003A and K2046A mutations in *BEM2* (Figure 3A). Both mutant alleles were expressed at levels comparable to those of the wild-type Bem2p (Figure 2B). The morphogenesis phenotype of these mutants was qualitatively similar to that of *bem2*Δ mutants, though not quite as penetrant or as severe (Figure 2C and D). However, the mutant strains were fully capable of enacting a checkpoint-mediated cell cycle arrest in response to Lat-B (Figure 2E). This result suggests that GAP activity is important for the morphogenesis role, but not for the checkpoint role, of Bem2p.

The interpretation of this experiment relies on whether or not the mutations impaired the GAP activity of Bem2p. Although a strong argument that they must do so can be made based on structural considerations, we wished to confirm that this was indeed the case. To that end, we made recombinant GST fusion proteins containing the GAP domain of wild-type or mutant Bem2p. The physiological target Rho proteins for this domain are not entirely clear. Previous studies indicated that the Bem2p GAP domain could act on Rho1p *in vitro*, although the phenotype of *bem2* mutants is more suggestive of an involvement with the polarity establishment GTPase Cdc42p *in vivo*. We have had some success in measuring Cdc42p-directed GAP activity associated with Rga1p (Gladfelter *et al*., 2002), and we found that the Bem2p GAP domain was also effective in accelerating GTP hydrolysis by Cdc42p (Figure 3B). Using this assay, we found that both of the mutations described above greatly reduced the *in vitro* GAP activity of GST–Bem2p (Figure 3). Thus, we feel confident that Bem2p GAP activity is impaired by the mutations, and therefore that GAP activity of Bem2p is not required for the morphogenesis checkpoint.

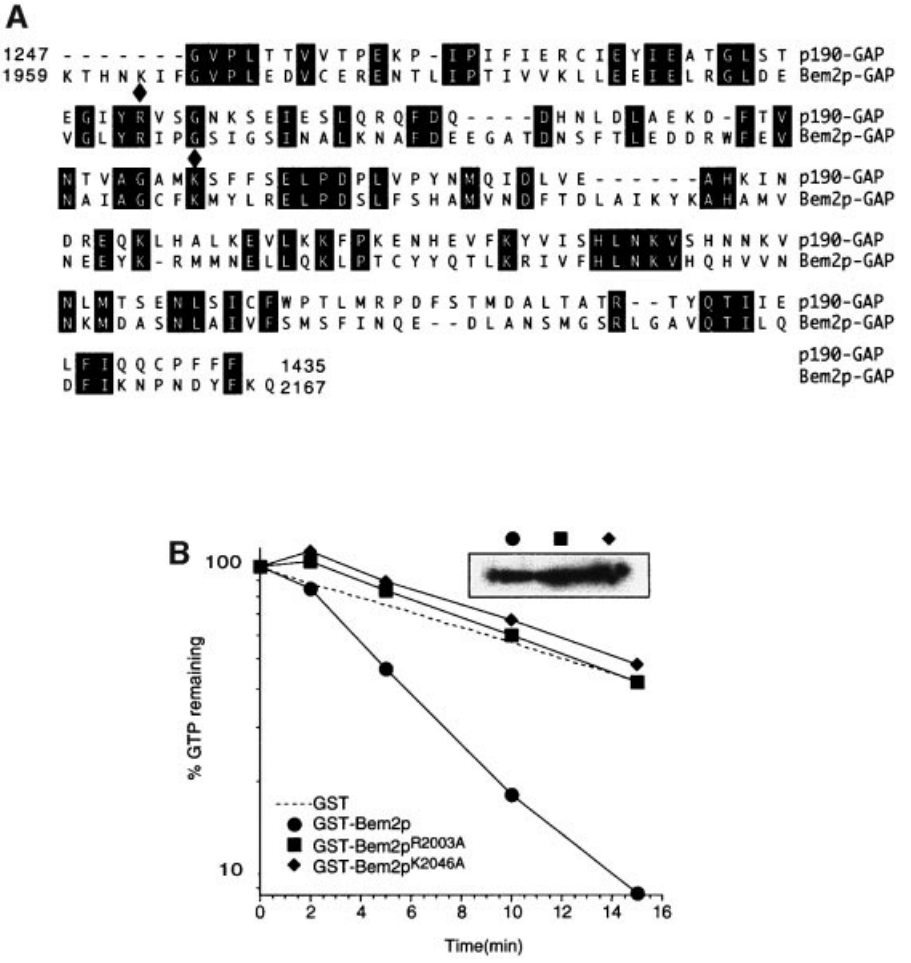

Fig. 3. Point mutations in Bem2p greatly reduce GAP activity. (**A**) Alignment of the Bem2p and mammalian p190 GAP domains. Residues of Bem2p homologous to critical residues of p190 are indicated by filled diamonds. (**B**) Cdc42p prebound to [γ-^{32}P]GTP was incubated with GST, GST–Bem2 GAP domain, or the same domain with the R2003A or K2046A change. Radioactivity remaining bound to Cdc42p is plotted against time of incubation. The inset shows an anti-GST western blot indicating that equal levels of the different GAP domains were used in each assay. Control experiments with Cdc42p bound to [α-^{32}P]GTP did not show a decline in bound radioactivity, demonstrating that the observed decrease reflected GTP hydrolysis, not release of GTP (data not shown).

Uncoupling the morphogenesis and checkpoint roles of Bem2p

Previous studies showed that the morphogenesis defects of *bem2* mutants could be largely suppressed by a dominant mutation causing the expression of a truncated derivative of the Cdc42p-GAP Rga1p, which retained the GAP domain but lacked an N-terminal region containing two LIM domains (Chen *et al*., 1996). This result, combined with some shared phenotypes between *rga1* and *bem2* mutants, and the finding that *rga1*Δ *bem2*Δ double mutants were inviable, led Chen and colleagues to conclude that these two Rho-GAPs shared some function(s) in morphogenesis. We confirmed that overexpression of N-terminally truncated *RGA1* could effectively suppress the morphology defect of *bem2*Δ mutants in our strain background (Figure 4A). However, the truncated *RGA1* was completely unable to restore checkpoint function to the *bem2*Δ mutant (Figure 4B). This strain therefore uncouples the morphogenesis defect from the checkpoint defect, strongly suggesting that the checkpoint defect is not an indirect effect of the perturbation of morphogenesis, but rather represents a separate function of Bem2p.

Mutational analysis of the N-terminal domain of Bem2p

As the GAP activity of Bem2p was not required for its checkpoint role, we investigated the large non-catalytic N-terminal portion of the protein. Apart from a potential pleckstrin homology (PH) domain adjacent to the GAP domain at the C-terminus, this region does not display obvious sequence motifs, with the possible exception of a short hydrophobic stretch (residues 688–707), which could be a transmembrane domain (Figure 5A). We made a series of low-copy plasmids that express wild type or N-terminally truncated derivatives of Bem2p from its own promoter, containing a C-terminal myc tag for ease of detection. These derivatives were expressed at levels roughly comparable to those of full-length Bem2p-myc, suggesting that they encode stable proteins (Figure 5B). When the plasmids were introduced into a *bem2*Δ strain, we found that removal of the first 237 amino acids did not affect the ability of the Bem2p derivative to complement either the morphogenesis defect (Figure 5C) or the checkpoint defect (Figure 5D) of the mutant. However, removal of the first 695 amino acids (or more) eliminated

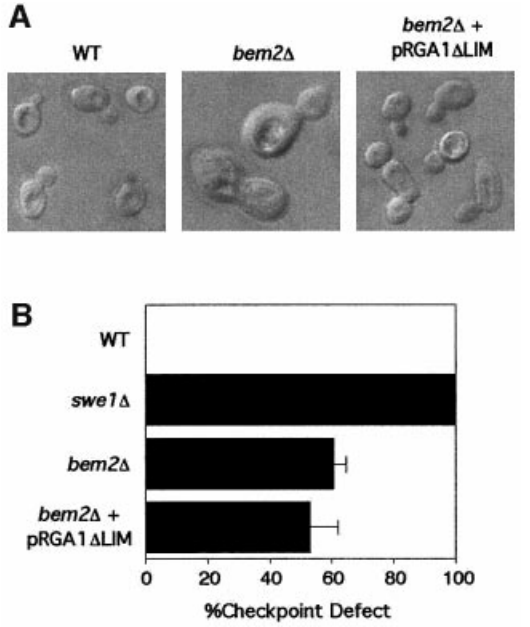

Fig. 4. Effect of overexpression of *RGA1*ΔLIM on cell morphology and checkpoint function in *bem2*Δ cells. (**A**) The strains DLY1 (*BEM2*) and DLY 4015 (*bem2*Δ) containing either empty plasmid (YEplac195) or *RGA1*ΔLIM (pDLB2129) were grown to exponential phase in dextrose-containing medium at 30°C. Images of live cells were captured using DIC microscopy. (**B**) The indicated strains were assayed for checkpoint function as in Figure 2A.

complementation of both defects (Figure 5C and D). Amino acid 695 is centered in the middle of the putative transmembrane domain, and we found that a small internal deletion lacking amino acids 688–707 was also unable to complement *bem2*Δ phenotypes (Figure 5C and D).

These results suggested that the putative transmembrane domain was required for proper Bem2p function, and raised the possibility that Bem2p might indeed be an integral membrane protein. To test whether this was the case, we separated a cell lysate of a strain expressing Bem2p-myc into membrane and soluble fractions by high-speed centrifugation. Whereas the control integral membrane proteins Sso1/2p were found in the pellet, Bem2p was quantitatively retained in the supernatant fraction (Figure 5E), showing that it is not an integral membrane protein. Presumably the hydrophobic region of Bem2p is serving some other essential function, either by interacting with other components or by mediating proper folding of the protein. Thus far, we have not succeeded in isolating a *bem2* derivative that is defective with regard to the checkpoint function but not with regard to morphogenesis.

Bem2p levels during the cell cycle and in response to Lat-B

In order to determine the expression of Bem2p during the cell cycle, we arrested cells containing Bem2p-myc in G_1, S or G_2/M, and compared the level of Bem2p protein to that in asynchronous cells. The abundance of Bem2p did not differ significantly at different stages of the cell cycle (Figure 6). Similarly, cells that had been exposed to Lat-B did not show a significant difference in the level of Bem2p (Figure 6). Thus, if Bem2p is itself regulated by cell cycle or checkpoint cues, this regulation does not appear to be at the level of total abundance of Bem2p.

Stabilization of Swe1p in bem2Δ mutants treated with Lat-B

One effect of actin perturbation is the stabilization and consequent accumulation of Swe1p (Sia *et al*., 1998). Surprisingly, we found that proliferating *bem2*Δ cells expressed slightly higher amounts of Swe1p than wild-type controls (Figure 7A). Furthermore, Swe1p abundance was increased in *bem2*Δ mutants exposed to Lat-B, to levels equal to or exceeding those observed in wild-type cells exposed to Lat-B (Figure 7A). This result suggests that *bem2*Δ cells do not have a defect in Swe1p stabilization. Swe1p degradation requires the kinase Hsl1p, and in *hsl1*Δ mutants Swe1p is constitutively stable. We found that even *bem2*Δ *hsl1*Δ double mutants, in which Swe1p is presumably stable, failed to arrest the cell cycle in response to Lat-B (Figure 7B). We conclude that the checkpoint defect of *bem2*Δ mutants is not due to a failure to stabilize Swe1p.

Activation of Mpk1p in bem2Δ mutants treated with Lat-B

A second effect of actin perturbation is the activation of a kinase cascade culminating in the MAPK Mpk1p, which is required to arrest the cell cycle in response to Lat-B, probably through inhibition of the phosphatase Mih1p (Harrison *et al*., 2001). Activation of Mpk1p can be monitored using an antibody that detects only the doubly phosphorylated (active) form of the protein. Using this reagent, we found that activation of Mpk1p in response to Lat-B occurred equally well in wild-type and in *bem2*Δ cells (Figure 7C). We conclude that the checkpoint defect of *bem2*Δ mutants is not due to a failure to activate Mpk1p.

Mih1p in bem2Δ mutants

One possible reason for the *bem2*Δ checkpoint defect would be that *bem2*Δ mutants fail to inhibit the phosphatase Mih1p. We found that there was an equivalent amount of Mih1p in wild-type and *bem2*Δ cells (Figure 7D), but this result does not rule out an effect of Bem2p on Mih1p activity. If the checkpoint defect of *bem2*Δ cells was due to a lack of Mih1p inhibition, then deleting *MIH1* should eliminate the need for such inhibition, thereby making Bem2p unnecessary for proper checkpoint function. Deletion of *MIH1* did partially rescue the *bem2*Δ checkpoint defect (Figure 7E), consistent with a role of Bem2p in Mih1p regulation. However, the fact that there was still a partial checkpoint defect in the *bem2*Δ *mih1*Δ strain suggests that Bem2p must also have an Mih1p-independent role in checkpoint function.

Cdc28p phosphorylation in bem2Δ mutants treated with Lat-B

As the experiments described above indicated that the known morphogenesis checkpoint pathways were intact in the *bem2*Δ mutant, we wondered whether this mutant would be able to induce the inhibitory phosphorylation at Cdc28p Tyr19 in response to Lat-B. This phosphorylation can be readily detected using a phospho-epitope-specific antibody. We found that basal levels of Cdc28p phosphorylation were elevated in *bem2*Δ cells (Figure 7F),

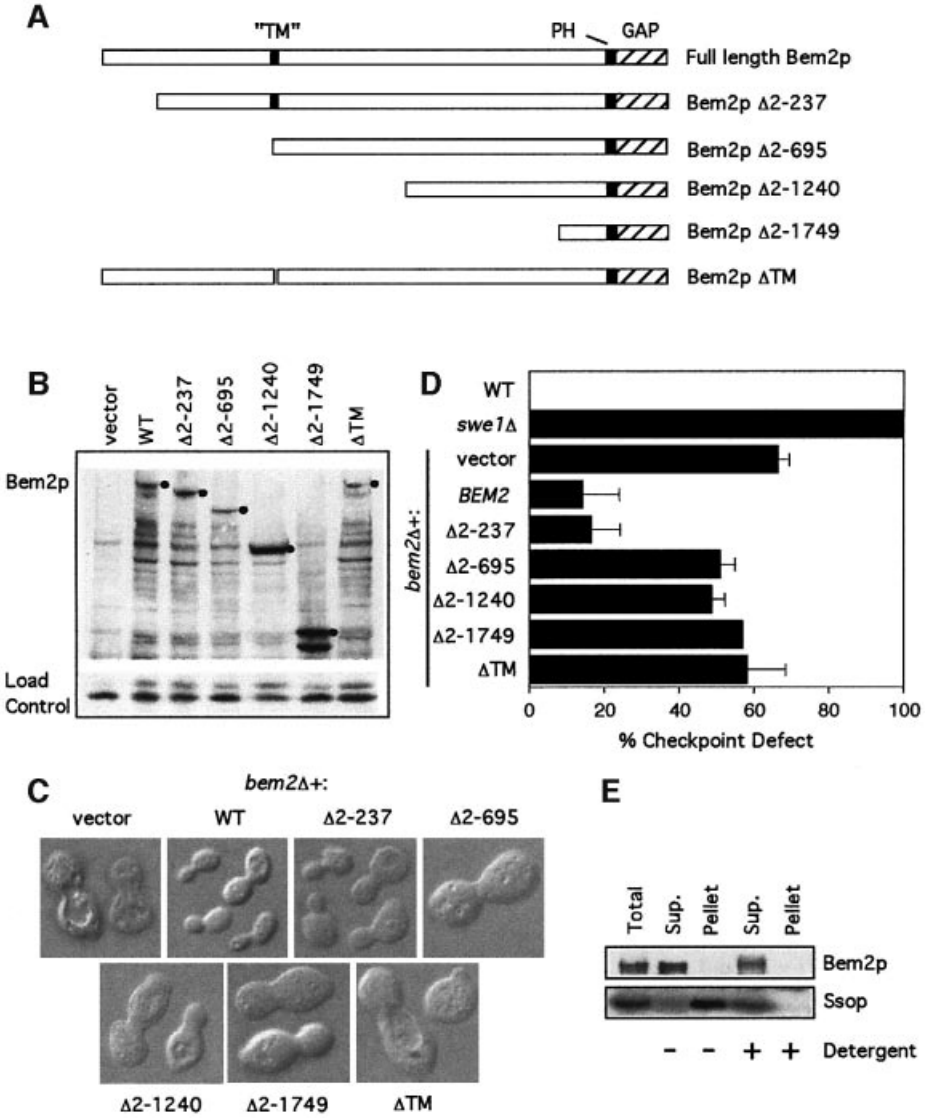

Fig. 5. Deletion anaylsis of the N-terminal domain of Bem2p. (**A**) Domain structure of Bem2p, showing the C-terminal GAP domain, the PH domain and the putative transmembrane (TM) domain. Also illustrated are the regions of the protein missing in the various deletion constructs. (**B**) The *bem2*Δ strain DLY4015 containing the plasmids pRS316 (vector), pDLB768 (WT), pDLB2147 (Δ2–237), pDLB2118 (Δ2–695), pDLB2116 (Δ2–1240), pDLB2115 (Δ2–1749) or pDLB2249 (ΔTM) was grown to exponential phase in dextrose-containing media. Cell lysates from these strains were immunoblotted with an anti-myc antibody. The bands corresponding to full-length protein for each construct are marked with a filled circle. (**C**) Images of live cells from the same strains were captured using DIC microscopy. (**D**) The indicated strains were assayed for checkpoint function as in Figure 2A. (**E**) Cells of strain DLY4860 (*BEM2-myc*) were lysed and fractionated by ultracentrifugation at 250 000 *g* for 1 h. Pellet fractions were resuspended to the same volume as the supernatant and equal volumes were analyzed by immunoblotting with α-myc and α-Sso1/2p antibodies.

perhaps due to the increased basal level of Swe1p (Figure 7A). However, *bem2*Δ cells were severely attenuated in their ability to phosphorylate Cdc28p in response to Lat-B (Figure 7F). Thus, it appears that *bem2*Δ cells are incapable of effectively phosphorylating Cdc28p, despite their ability to stabilize Swe1p and activate Mpk1p. This defect presumably accounts for their inability to arrest the cell cycle in response to actin perturbation.

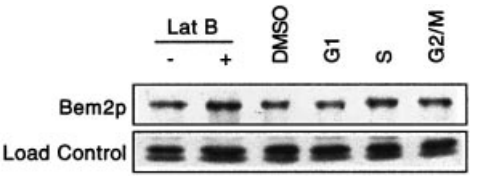

Fig. 6. Bem2p levels through the cell cycle and following treatment with Lat-B. The strain DLY4860 (*BEM2-myc*) was grown to exponential phase in YEPD at 30°C and then treated with 100 μM Lat-B, 30 ng/ml α-factor (G_1), 0.25 M hydroxyurea (S) or 15 μg/ml nocodazole (G_2/M) as indicated. Cells were then lysed and immunoblotted with an α-myc antibody.

Discussion

How is bud formation monitored by the morphogenesis checkpoint?

The process of bud formation begins with the inheritance by newborn cells of spatial landmarks that specify the future site of bud emergence (reviewed by Pringle *et al.*, 1995; Pruyne and Bretscher, 2000a,b). These landmarks are then 'interpreted' by the GTPase Rsr1p and its regulators Bud2p and Bud5p, which promote localization

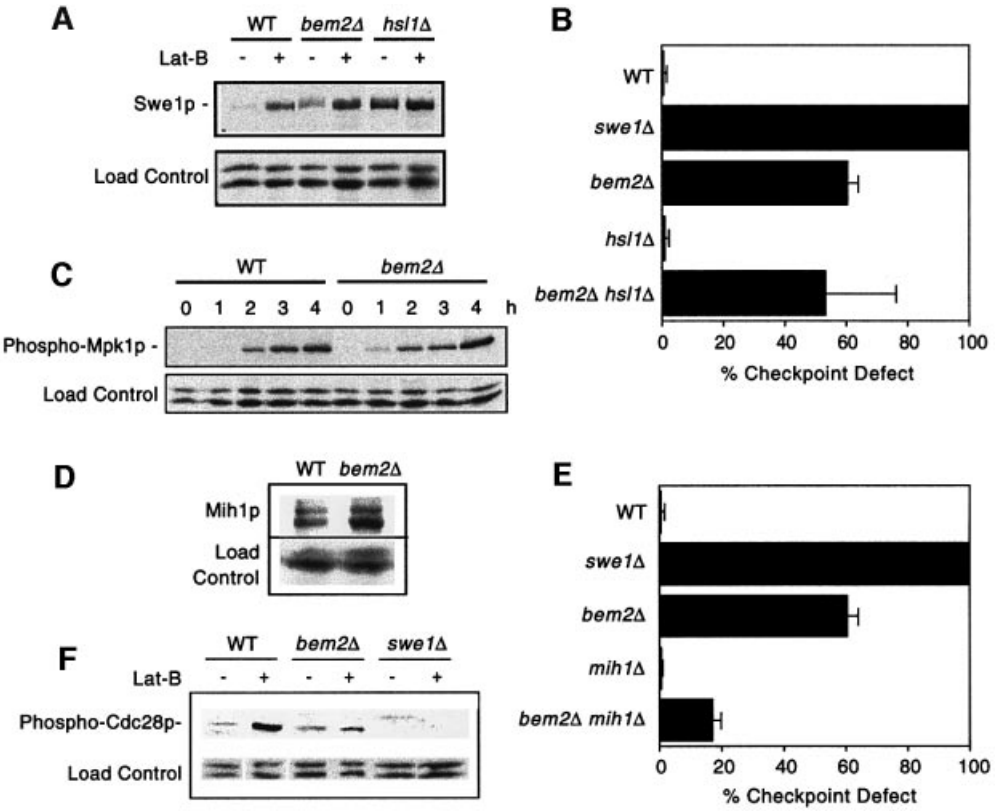

Fig. 7. Swe1p, Mpk1p and Cdc28p regulation in *bem2*Δ cells. (**A**) The strains DLY1 (WT), DLY4021 (*swe1*Δ), DLY4015 (*bem2*Δ), JMY3-1 (*hsl1*Δ) and DLY4019 (*bem2*Δ *hsl1*Δ) were assayed for checkpoint function as in Figure 2A. (**B**) The strains DLY5330 (*SWE1-myc*), DLY5331 (*bem2*Δ *SWE1-myc*) and JMY1503 (*hsl1*Δ *SWE1-myc*) were grown to exponential phase and then resuspended in 100 μM Lat-B in YEPD and cultured for 2 h at 30°C. Lysates from cells before and after growth in Lat-B were immunoblotted with α-myc antibody. (**C**) The strains DLY1 (WT) and DLY4015 (*bem2*Δ) were grown to exponential phase in YEPD + 0.4 M NaCl, followed by resuspension and growth for the indicated times in the same medium supplemented with 100 μM Lat-B. Lysates were immunoblotted with anti-phospho-p44/p42 MAPK antibody to detect activated Mpk1p. (**D**) The strains JMY1299 (*MIH1-myc*) and DLY 4478 (*bem2*Δ *MIH1-myc*) were grown to exponential phase. Lysates were immunoblotted with α-myc antibody. (**E**) The strains DLY1 (WT), DLY4021 (*swe1*Δ), DLY4015 (*bem2*Δ), JMY3-59 (*mih1*Δ) and DLY3860 (*bem2*Δ *mih1*Δ) were assayed for checkpoint function as in Figure 2A. (**F**) The strains DLY1 (WT), DLY4015 (*bem2*Δ) and DLY4021 (*swe1*Δ) were grown to exponential phase in YEPD at 24°C and then resuspended in 100 μM Lat-B in YEPD and cultured for an additional 2 h. Lysates from cells before and after growth in Lat-B were immunoblotted with an anti-phospho-cdc2 antibody to visualize Tyr19 phosphorylated Cdc28p.

of polarity establishment proteins, including Cdc24p and Cdc42p, to the appropriate site. The Cdc42p GTPase and its effectors then cause polarization of actin structures towards that site and assembly of a septin ring at that site. Polarized secretion directed by actin cables and local cell wall deposition by septin-associated proteins then collaborate to promote bud emergence. Reasoning that the checkpoint would probably monitor some structure involved in bud formation, we tested whether mutations in the genes encoding spatial landmarks, Rsr1p and its regulators, polarity establishment proteins, actin cytoskeletal proteins, or septins would cause a checkpoint defect. With the sole exception of *bem2* mutants (and even in that case, many checkpoint pathways remained intact; see below), all of these strains were competent to arrest the cell cycle in response to Lat-B. This situation appears quite different from that described for the DNA replication and spindle assembly checkpoints, where mutations that affect early steps in the process (assembly of replication forks or kinetochores, respectively) preclude checkpoint function (Piatti *et al*., 1995; Gardner *et al*., 2001).

One possibility for what might be monitored by the morphogenesis checkpoint is the concentration of monomeric G-actin. The ability of actin depolymerization by Lat-B to trigger a checkpoint response in many mutant strains is consistent with this hypothesis. Conceivably, mutations and environmental stresses that delay bud formation might all increase the G-actin concentration, which would make this a useful parameter to monitor (a transient increase in G-actin has been reported following thermal or osmotic shock) (Yeh and Haarer, 1996). If that were the case, then we reasoned that interaction of G-actin with the hypothetical sensor would be critical for checkpoint sensing. Wertman *et al*. (1992) have generated a panel of clustered charged-to-alanine scanning mutations across the entire *ACT1* gene, which are expected to disrupt interactions with the surface of actin. However, none of the viable alleles in this series disrupted checkpoint function (Table I), and we were unable to obtain any experimental support for this hypothesis.

Another possibility is that the checkpoint does indeed monitor some aspect of bud emergence, but that rather than emitting a 'wait' signal when bud emergence is impaired, the checkpoint emits an 'all-clear' signal when bud emergence is successful. Consistent with this hypothesis, it appears that degradation of Swe1p requires its

targeting to the bud side of the mother-bud neck, a location that only exists following successful bud emergence (Longtine *et al*., 2000). If it is successful bud emergence that triggers Swe1p degradation and subsequent cell cycle progression, then a failure of bud emergence would automatically lead to Swe1p accumulation and cell cycle delay, regardless of whether mutations impaired early or late steps in bud emergence. However, it should be noted that severe actin depolymerization can cause a Swe1p-mediated arrest even after cells have made a bud, so the checkpoint cannot only respond to bud emergence (McMillan *et al*., 1998).

How many pathways are involved in the morphogenesis checkpoint arrest?

In addition to stabilization and accumulation of Swe1p (Sia *et al*., 1998), previous work indicated that an effective checkpoint arrest required activation of a kinase cascade culminating in the MAPK Mpk1p/Slt2p, which is thought to act by inhibiting the phosphatase Mih1p (Harrison *et al*., 2001). In this report we have shown that the Rho-GAP Bem2p is also required for an effective checkpoint arrest. Surprisingly, lack of Bem2p did not affect either Swe1p accumulation or Mpk1p activation, suggesting that a minimum of three independent pathways collaborate to induce a checkpoint arrest in response to Lat-B. As Bem2p abundance was unaffected by the checkpoint, it is not yet clear whether Bem2p actively participates in a regulated checkpoint pathway or whether constitutive Bem2p is required to allow the function of a checkpoint pathway.

Why would the checkpoint require several pathways? One possibility is that instead of having a single checkpoint sensor, the morphogenesis checkpoint integrates information from multiple sensors to calibrate the appropriate response. For instance, it may be that Swe1p degradation responds to signals emanating in the vicinity of the septins at the mother-bud neck (Barral *et al*., 1999; Longtine *et al*., 2000), whereas Mpk1p responds to the status of the plasma membrane (Kamada *et al*., 1995) and Bem2p responds to yet another signal. Only when perturbations affected a combination of these sensors would cells mount a checkpoint response.

Regardless of whether one or several sensors are required to trigger the checkpoint, the collaboration of several independent pathways impinging on the cell cycle machinery may be essential to achieve an effective arrest. Indeed, it is clear that neither stabilization of Swe1p nor inhibition of Mih1p is sufficient to produce a prolonged cell cycle delay, although together they are quite effective (McMillan *et al*., 1999). Given the precedents in other systems for control of Swe1p/Mih1p homologs by post-translational means (Kumagai and Dunphy, 1992; Coleman *et al*., 1993; Parker *et al*., 1993; Wu and Russell, 1993; Mueller *et al*., 1995; Furnari *et al*., 1997; Lee *et al*., 2001), it seems likely that Bem2p is required for either activation of Swe1p or inhibition of Mih1p under checkpoint conditions. The *bem2*Δ checkpoint defect cannot be entirely accounted for by a role for Bem2p in Mih1p inhibition, because *bem2*Δ *mih1*Δ mutants are still partially defective for checkpoint-mediated arrest. Thus, we favor the hypothesis that Bem2p acts to stimulate Swe1p activity, and that without this stimulus the Swe1p that accumulates upon Lat-B treatment is unable to effectively phosphorylate Cdc28p and cause G_2 arrest. Future studies will test this hypothesis by developing a quantitative assay for Swe1p specific activity.

Rho-GAP-dependent and Rho-GAP-independent roles for Bem2p

Cells lacking Bem2p have a complex phenotype that includes defects in actin polarity (Wang and Bretscher, 1995), bud site selection (Kim *et al*., 1994), cell wall integrity (Cid *et al*., 1998) and septin organization (Cid *et al*., 2001), as well as the morphogenesis checkpoint defect described here. As Rho-GTPases participate in all of these processes (Pringle *et al*., 1995; Ridley, 1995; Cabib *et al*., 1998; Harrison *et al*., 2001; Gladfelter *et al*., 2002), the *bem2*Δ defects could simply stem from an increase in the concentration of GTP-bound Rho proteins in the cell. However, we found that GAP-defective *bem2* alleles were still competent to perform Bem2p's checkpoint role. Conversely, while expression of a deregulated Rga1p Rho-GAP effectively suppressed the *bem2*Δ morphology defect, it could not restore checkpoint function to *bem2*Δ mutants. Together, these results argue that the Bem2p checkpoint function is separate from its Rho-GAP activity.

Rho-GAP domains are generally found in large proteins that often contain additional recognizable domains, including PH domains (Furukawa *et al*., 2001; Krugmann *et al*., 2002; Miura *et al*., 2002), GEF domains (Chuang *et al*., 1995), Arf-GAP domains (Krugmann *et al*., 2002; Miura *et al*., 2002), LIM domains (Chen *et al*., 1996), SH3 domains (Furukawa *et al*., 2001), WW domains (Furukawa *et al*., 2001) and even in one case a myosin motor (Wirth *et al*., 1996). However, the purpose of having these various domains in the same protein is unclear. It has been speculated that the additional domains are important for the regulation of GAP activity or localization of the GAP to different complexes within the cell (Watanabe *et al*., 2001), but the existence of such links has yet to be demonstrated. Our results with Bem2p suggest that it too must have at least one additional functional domain that acts in the morphogenesis checkpoint. The nature of that domain and the link, if any, between the Bem2p checkpoint function and its Rho-GAP function remains to be determined.

Materials and methods

Yeast strains and plasmids

Standard genetic and molecular biology methods were used to generate all strains and plasmids used in this study, except as indicated below. The yeast strains used are listed in Table II. The oligonucleotides used are listed in Table III. The *swe1::TRP1* (Harrison *et al*., 2001), *hsl1-Δ1::URA3* (Ma *et al*., 1996), *SWE1-myc::HIS2* (McMillan *et al*., 1999), *bem1::URA3* (Chenevert *et al*., 1992), *spa2::URA3* (Gehrung and Snyder, 1990), *msb1::URA3* (Bender and Pringle, 1991), *cla4::TRP1* (Benton *et al*., 1997), *ste20::TRP1* (Leberer *et al*., 1992), *abp1::URA3* (Adams *et al*., 1993), *tpm1::URA3* (Liu and Bretscher, 1989), *sac6::LEU2* (Adams *et al*., 1991) and *cap2::URA3* (Amatruda *et al*., 1990) alleles were all generated as described previously. The *pfy1-111::LEU2* allele (Haarer *et al*., 1993) was serially backcrossed six times into the BF264-15DU background.

The *bem2::TRP1*, *bem2::URA3*, *bem2::LEU2*, *mih1::TRP1*, *rho4::TRP1*, *bud5::LEU2*, *rsr1::URA3*, *myo3::TRP1*, *myo4::URA3* and *myo5::URA3* alleles were constructed by the one-step PCR method (Baudin *et al*., 1993) with plasmids pRS304 (TRP1), pRS305 (LEU2) or pRS306 (URA3) (Sikorski and Hieter, 1989) as templates. The PCR

Table II. Yeast strains used in this study

Strain name	Relevant genotype	Source
BHY31	**a** *pfy1-112::LEU2*	Haarer *et al.* (1993)
BHY32	**a** *pfy1-116::LEU2*	Haarer *et al.* (1993)
BY4743[a]	**a**/α	Research Genetics
CCY1042-12B	α *gic1-Δ1::LEU2 gic2-Δ2::TRP1*	Bi *et al.* (2000)
DBY7055	**a** *aip3Δ2::HIS3*	Amberg *et al.* (1997)
DDY336	**a** *act1-133::HIS3*	Wertman *et al.* (1992)
DDY337	**a** *act1-108::HIS3*	Wertman *et al.* (1992)
DDY338	**a** *act1-101::HIS3*	Wertman *et al.* (1992)
DDY339	**a** *act1-102::HIS3*	Wertman *et al.* (1992)
DDY340	α *act1-104::HIS3*	Wertman *et al.* (1992)
DDY341	**a** *act1-111::HIS3*	Wertman *et al.* (1992)
DDY343	α *act1-115::HIS3*	Wertman *et al.* (1992)
DDY344	α *act1-116::HIS3*	Wertman *et al.* (1992)
DDY346	**a** *act1-119::HIS3*	Wertman *et al.* (1992)
DDY347	**a** *act1-120::HIS3*	Wertman *et al.* (1992)
DDY348	**a** *act1-123::HIS3*	Wertman *et al.* (1992)
DDY349	α *act1-124::HIS3*	Wertman *et al.* (1992)
DDY351	α *act1-129::HIS3*	Wertman *et al.* (1992)
DDY352	**a** *act1-132::HIS3*	Wertman *et al.* (1992)
DDY353	α *act1-135::HIS3*	Wertman *et al.* (1992)
DDY356	α *act1-105::HIS3*	Wertman *et al.* (1992)
DDY357	**a** *act1-115::HIS3*	Wertman *et al.* (1992)
DDY654	α *act1-121::HIS3*	Wertman *et al.* (1992)
DDY655	**a** *act1-122::HIS3*	Wertman *et al.* (1992)
DDY1253	α *cof1-4::LEU2*	Lappalainen *et al.* (1997)
DDY1254	α *cof1-5::LEU2*	Lappalainen *et al.* (1997)
DDY1266	α *cof1-22::LEU2*	Lappalainen *et al.* (1997)
DLY1	**a** *bar1*	Sia *et al.* (1996)
DLY657	**a** *bar1 cdc24-1*	Sia *et al.* (1996)
DLY2609	**a** *bar1 sac6::LEU2*	This study
DLY2736	**a** *bar1 bud5::LEU2*	This study
DLY3368	**a** *bar1 rsr1::URA3*	This study
DLY3860	**a** *bar1 bem2::URA3 mih1::TRP1*	This study
DLY3966	**a** *bar1 rho4::TRP1*	This study
DLY4015	**a** *bar1 bem2::TRP1*	This study
DLY4019	**a** *bar1 bem2::TRP1 hsl1::URA3*	This study
DLY4021	**a** *bar1 swe1::TRP1*	Harrison *et al.* (2001)
DLY4478	**a** *bar1 bem2::TRP1 MIH1-myc::URA3*	This study
DLY4497	**a** *bar1 rho2::KAN^r*	Harrison *et al.* (2001)
DLY4860	**a** *bar1 BEM2-myc::URA3*	This study
DLY4862	**a** *bar1 bem2K2046A-myc::URA3*	This study
DLY5041	**a** *bar1 bem2R2003A-myc::URA3*	This study
DLY5330	**a** *bar1 SWE1-myc::HIS2*	This study
DLY5331	**a** *bar1 bem2::TRP1 SWE1-myc::HIS2*	This study
DLY5516[a]	**a**/α *bem2::KanMX/bem2::LEU2*	This study
JMY2-13	**a** *bar1 abp1::URA3*	This study
JMY2-14	**a** *bar1 spa2::URA3*	This study
JMY2-15	**a** *bar1 msb1::URA3*	This study
JMY2-26	**a** *myo2-66*	McMillan *et al.* (1998)
JMY3-1	**a** *bar1 hsl1::URA3*	This study
JMY3-59	**a** *bar1 mih1::TRP1*	This study
JMY1011	**a** *bar1 bem1::URA3*	This study
JMY1020	**a** *tpm1::URA3*	This study
JMY1023	**a** *cap2::URA3*	This study
JMY1066	**a** *pfy1-111::LEU2*	This study
JMY1237	**a** *myo5::URA3*	This study
JMY1239	α *myo4::URA3*	This study
JMY1250	α *myo3::TRP1*	This study
JMY1299	**a** *bar1 MIH1-myc::URA3*	This study
JMY1503	**a** *bar1 hsl1::URA3 SWE1-myc::HIS2*	McMillan *et al.* (1999)
JPT194-H01	**a**/α *cdc11-6/cdc11-6*	John Pringle
LH17012-H01	**a**/α *cdc10-1/cdc10-1*	John Pringle
MOSY148	**a** *cla4::TRP1*	This study
MOSY150	**a** *ste20::TRP1*	This study
RNY140	**a** *myo1::KAN^r*	John Pringle
YBR260CΔ[a]	**a**/α *rgd1::KanMX/rgd1::KanMX*	Research Genetics
YDL240WΔ[a]	**a**/α *lrg1::KanMX/lrg1::KanMX*	Research Genetics
YDR379WΔ[a]	**a**/α *rga2::KanMX/rga2::KanMX*	Research Genetics
YDR389WΔ[a]	**a**/α *sac7::KanMX/sac7::KanMX*	Research Genetics
YEF369	**a** *bud2::TRP1*	John Pringle
YEF395	**a**/α *bud1::HIS3/bud1::HIS3 bud8::HIS3/bud8::HIS3*	John Pringle
YEF1269	**a** *msb3Δ::HIS3 msb4Δ::HIS3*	Bi *et al.* (2000)

Table II. *Continued*

Strain name	Relevant genotype	Source
YFL047WΔ[a]	**a/α** *yfl047w::KanMX/yfl047w::KanMX*	Research Genetics
YHR182WΔ[a]	**a/α** *yhr182w::KanMX/yhr182w::KanMX*	Research Genetics
YJL187CΔ[a]	**a/α** *swe1::KanMX/swe1::KanMX*	Research Genetics
YJL201WΔ[a]	**a/α** *yjl201w::KanMX/yjl201w::KanMX*	Research Genetics
YJZ427	**a** *bni1Δ::HIS3*	Zahner *et al.* (1996)
YOR127WΔ[a]	**a/α** *rga1::KanMX/rga1::KanMX*	Research Genetics
YOR134WΔ[a]	**a/α** *bag7::KanMX/bag7::KanMX*	Research Genetics
YPL115CΔ[a]	**a/α** *bem3::KanMX/bem3::KanMX*	Research Genetics

[a]Strains obtained from Research Genetics (and DLY5516, which was derived from the *bem2*Δ Research Genetics strain which was found to be heterozygous for the *bem2*Δ deletion) are in the BY4743 background (*his3Δ1/his3Δ1 leu2Δ0/leu2Δ0 ura3Δ0/ura3Δ0 lys2Δ0/*LYS2 *met15Δ0Δ/*MET15). All other strains generated in this study are in the BF264-15DU (Richardson, 1989) background (*ade1 his2 leu2-3 112 trp1-1*[a] *ura3Δns*).

Table III. Oligonucleotides used in this study

Oligo name	Oligonucleotide sequence
ARMO1	GGAATTCCATATGAAAACTCATAATAAGATATTTGGGGTACC
ARMO2	CCGAGCTCTTATTGCTTGAAATAATCATTTGGATTC
ARMO3	GTCTAATGAAAGGTCTTCTCTGGTCTAAGAACAGGAAATCTTCAACGGCCGCGCGTTTCGGTGATGAC
ARMO4	TTATTGCTTGAAATAATCATTTGGATTTGGATTCTTAATAAAATCTTGCAGGATTTTCCTGATGCGGTATTTTCTCCT
ARMO6	GAAGTGGGATTGTACGCGATTCCTGGTTCCA
ARMO7	TGGAACCAGGAATCGCGTACAATCCCACTTC
ARMO8	GCGATCGCAGGCTGTTTCGCGATGTATTTAAGAGAG
ARMO9	CTCTCTTAAATACATCGCGAAACAGCCTGCGATCGC
ARMO33	AGATCTTCATTAGACTCCTGCTTCGTTCGTTATTTG
BUD5-1	GCATGAGAACGGCCGTACCGCAGTTGCTGGAAGCAACTGCCTGTGTCTCTAGGCGCGTTTCGGTGATGA
BUD5-2	GTTTTTAGGTAAGCCTTGGAACCTTAGCTATACTGACTTGATACGCCCTTTCCTGATGCGGTATTTTCTCCT
H16	GCTCTAGAGGCTTACTACTATGCGTTCAA
H17	CGAGTCGACTTGCTTGAAATAATCATTTGG
OJ17	TGGACAAACCAGGATTGAAGTCAGCGAGGGTGAAGAAACCGCGCGTTTCGGTGATGAC
OJ18	ATTAACGATCTTCTTGCGGGCCTGGGTAAATCTTCTCGGTTTTCCTGATGCGGTATTTTCTCCT
OJ37	CAATCCAGTTATAAAACATTAATTTGCTGATCACATTTGAATCGCGCGTTTCGGTGATGAC
OJ38	GTCATCATCATCATCGCCATCGTCATTATCATCATCGTCATTTCCTGATGCGGTATTTTCTCCT
OJ39	CATGTCATTTGAAGTAGGAACTAAGTGTTGGTACCCTCACGCGCGTTTCGGTGATGAC
OJ40	CTGACAGTAGCTAAGCCCTCTGTATTGCTGTTCTGTGTTATTTCCTGATGCGGTATTTTCTCCT
OJ41	GCCAGCTAAACGCTCTGCGAATATCAAGAAAGCTACTTTTGCGCGTTTCGGTGATGAC
OJ67	CATGGAGACATTTAATAGACC
OJ68	CCATGAAATATCTCGAGCATGGTTTCTTCACCCTCGCTGAC
OJ69	GAAGAAACCATGCTCGAGATATTTCATGGAACTGAAG
OJ70	GAATTAGGATCCAGTGGACTGGATGACGCAGACG
RHO4-F	GTTACAGCAAACTTAAGTCAAATAGGTCCAAAAATCTCCAATAGTAACGCGCGCGTTTCGGTGATGAC
RHO4-R	GCCACTTTTCAAATGTTGTAAGTGCGTACAGAATGGGCAACAGAATAATCTTCTCCTGATGCGGTATTTTC
RSR1-2	GGACTAATGAGAGACTATAAATTAGTAGTATTGGGTGCTGGTGGTGTCGGGCGCGTTTCGGTGATGAC
RSR1-3	GTCTTTTTATCTGATATCTTGATTCATTTATAATAAAATTAAGTGACTTTTCCTGATGCGGTATTTTCTCCT
Z103	GACTCTGCAGAAAATTGTTCATTGGGAGCAGTTGATGC
Z105	GACTGAGCTCTTAGATTTGATATAATTAACGTGTGC
Z133	GACTCCGCGGCCATTAGACTCCTGCTTCGTTATTTG
Z134	GACTGAGCTCTCCACCTCCTTCCAGTTTAGGAGAGG
Z135	GACTGCTAGCCACATTAGACTCCTGCTTCGTTATTTG
Z136	GATCCATGGGACATTAGACTCCTGCTTCGTTATTTG
Z145	TATTGGATCCAAGTCATTTCCTGTCTTTAG
Z146	CCATGAAGATGACCTATGTTCAAATCTACAGCCAA
Z147	TTGGCTGTAGATTTGAACATAGGTCATCTTCATGG
Z148	AGAGGCGCGCGGATGATCTTGGAGGCGGCAAC

primers used were ARMO3 and ARMO4 for *BEM2*, OJ17 and OJ18 for *MIH1*, RHO4-F and RHO4-R for *RHO4*, BUD5-1 and BUD5-2 for *BUD5*, RSR1-2 and RSR2-3 for *RSR1*, OJ37 and OJ38 for *MYO3*, OJ39 and OJ40 for *MYO4*, and OJ41 and OJ42 for *MYO5*.

To create a myc-tagged version of the full-length *BEM2* gene, the 3′ end of the *BEM2* ORF was amplified with oligos H16 and H17. This PCR product was digested with *Xba*I and *Sal*I, and ligated into pSWE1-myc (McMillan *et al*., 1998) cut with *Xba*I and *Sal*I to excise the *SWE1* coding sequence. This creates pDLB1920, encoding an in-frame fusion of the 3′ end of *BEM2* and 12 myc tags. Digestion at the unique *Kpn*I site targets integration to the genomic *BEM2* locus, replacing endogenous *BEM2* with *BEM2*-12myc. Correct integration was confirmed by PCR and western blotting. A CEN plasmid expressing full-length BEM2-12myc from its own promoter was created by ligating a *Kpn*I–*Bam*HI fragment of pDLB1920 (encoding the 3′ end of *BEM2* and the myc tags) and a *Kpn*I–*Sma*I fragment of pCC554 (gift from C.Chan) into pRS316 (Sikorski and Hieter, 1989), which had been digested with *Not*I, blunted with Klenow enzyme and subsequently digested with *Bam*HI. The resulting plasmid, pDLB768, contains full-length *BEM2*-12myc with 995 bp of its own promoter followed by the ~500 bp *SWE1* terminator.

For expression of GST-tagged Bem2p GAP domain (amino acids 1958–2167) in bacteria, oligos ARMO1 and ARMO2 were used to amplify the GAP domain from genomic DNA, and the PCR product was cut with *Nde*I and *Sac*I and ligated into pUNI-10 (Liu *et al*., 1998),

creating pDLB1031. The R2003A and K2046A mutations were made by using overlap PCR with ARMO1 and ARMO2 as the flanking oligos, and either ARMO6 and ARMO7 (R2003A) or ARMO8 and ARMO9 (K2046A) as the internal oligos. These PCR products were similarly cloned into pUNI-10 with *Nde*I–*Sac*I, creating pDLB1609 (R2003A) and pDLB1699 (K2046A). All plasmids were sequenced to confirm that the expected mutations (and no others) were present. These plasmids were then recombined with pHB2-GST (Liu *et al*., 1998) (directing synthesis of proteins with GST fused to the N-terminus) to form pDLB1132 (WT), pDLB1705 (R2003A) and pDLB1721 (K2046A). The plasmid to express Cdc42p as a GST fusion in bacteria, pDLB2091, has been described previously (Gladfelter *et al*., 2002).

To integrate the point mutants of *BEM2* into the genome, a *Nde*I–*Sac*I fragment from each mutant in pUNI-10 and a *Kpn*I–*Bam*HI fragment from pDLB768 were used to GAP repair pDLB768 cut with *Eco*RI. The resulting plasmids, pDLB1772 (R2003A) and pDLB1773 (K2046A), were recovered and confirmed by restriction digest. A *Kpn*I–*Sal*I fragment spanning the mutation sites was used to replace the corresponding wild-type fragment in pDLB1920, yielding pDLB1921 (R2003A) and pDLB1922 (K2046A), which were then digested with *Kpn*I to target integration at *BEM2*. Correct integration was confirmed by PCR and western blotting.

To create a version of *RGA1* lacking the N-terminal LIM domains, oligos Z105 and Z103 were used to generate a PCR fragment containing 350 bp of the *RGA1* promoter along with the start codon, and this fragment was used to replace the *Sac*I–*Pst*I fragment from full-length *RGA1* (containing the promoter as well as the first 164 amino acids) in pDLB1537 (Gladfelter *et al*., 2002), yielding the 2 μm plasmid pDLB2129.

To create the *MIH1-myc::URA3* allele, a fragment containing the promoter region of *MIH1* was amplified using oligos OJ67 and OJ68, and cloned into pRS306 (Sikorski and Hieter, 1989) using *Kpn*I–*Xho*I. Then a second fragment containing the 5′ end of the *MIH1* gene was amplified with oligos OJ69 and OJ70, and cloned into the resulting plasmid using *Xho*I–*Bam*HI. The resulting plasmid was then linearized with *Xho*I and a 400 bp *Xho*I–*Sal*I fragment containing 12 tandem copies of the myc epitope (P.Russell, The Scripps Research Institute) was inserted. This creates pJM1030, which was linearized with *Bgl*II to target integration at *MIH1*, confirmed by PCR and western blotting.

The N-terminal deletion series of *BEM2* was created by using PCR to amplify a 650 bp region of the *BEM2* promoter along with the start codon, followed by various restriction sites. The 5′ oligo used to create these fragments was Z134. Fragments ending with *Nco*I (oligo Z136), *Nhe*I (oligo Z135), *Sac*II (oligo Z133) and *Bgl*II (oligo ARMO33) sites were amplified and ligated into pDLB768, which had been cut with *Sac*I and the appropriate second enzyme, creating plasmids that contained the *BEM2* promoter driving synthesis of Bem2p missing residues 2–237 (pDLB2147), 2–695 (pDLB2118), 2–1240 (pDLB2116) and 2–1749 (pDLB2115).

To create a *BEM2* plasmid missing amino acids 688–707, overlap PCR was used with internal oligos (Z146 and Z147) that loop out this region flanked by oligos (Z145 and Z148) that amplify an ~1 kb fragment. This fragment was cut with *Bam*HI and *Bss*HII and ligated into pDLB768, from which an analogous fragment was removed, creating the plasmid pDLB2249.

Media, growth conditions and cell synchrony

Yeast media (YEPD rich media, synthetic medium lacking specific nutrients and sporulation medium) have been described previously (Guthrie and Fink, 1991). Synchronous release of cells from α-factor arrest was carried out as described previously (McMillan *et al*., 1999). When indicated, log phase cultures (10^7 cells/ml) were resuspended in fresh medium containing 100 μM Lat-B (BioMol Research Laboratories Inc., Plymouth Meeting, PA) or 1% dimethylsulfoxide (DMSO; vehicle control).

Preparation of lysates and western blotting

Cell pelleting and lysis were carried out as previously described (McMillan *et al*., 1999). Detection of diphospho-Mpk1p and tyrosine phosphorylated Cdc28p has been described previously (Harrison *et al*., 2001). Detection of Sso1/2p was carried out as described previously (Lehman *et al*., 1999).

Morphogenesis checkpoint assay

The morphogenesis checkpoint assay has been described previously (Harrison *et al*., 2001).

Fluorescence staining and microscopy

To visualize nuclear DNA, cells were fixed in 70% ethanol for >1 h, harvested by centrifugation and resuspended in 0.3 μg/ml DAP (Sigma). Visualization of F-actin was accomplished by incubating fixed cells in 0.1 U/ml Alexa Fluor 568 phalloidin (Molecular Probes, Eugene, OR) for 20 min, followed by washing three times with PBS. Cells were then viewed on an Axioscop apparatus (Zeiss, Thornwood, NY) equipped with epifluorescence and differential interference contrast (DIC) optics. Images were captured using a cooled model charge-coupled device (CCD) camera (Princeton Instruments, Princeton, NJ).

Cell fractionation

Cell fractionation was carried out as described previously (Lehman *et al*., 1999), with the following modifications. To obtain sufficient levels of protein, 4.5×10^9 cells were harvested by centrifugation and washed in 3 ml of 10 mM Tris pH 7.5 and 10 mM sodium azide. Cells were then spheroplasted by incubation for 40 min in 7 ml of spheroplast buffer [0.1 mg/ml yeast lytic enzyme (ICN Biomedicals), 100 mM Tris pH 7.5, 10 mM sodium azide, 1.2 M sorbitol, 21 mM β-mercaptoethanol] at 37°C. Spheroplasts were then lysed in 3 ml of TEAE/sorbitol (10 mM TEA, 1 mM EDTA, 0.8 M sorbitol) with a 7 ml glass Dounce homogenizer. The homogenates were then cleared of intact cells and debris by centrifugation (450 *g*) for 30 min at 4°C. The supernatant was removed, divided into two and diluted 1:1 in either TEAE/sorbitol or TEAE/sorbitol/2% Triton X-100. The supernatant was then spun at 55 000 r.p.m. (250 000 *g*) in a TSL55 rotor for a Beckman l7-65 ultracentrifuge. All pellets were normalized to the volume of the supernatant fractions and 20 μl of each sample were run on an 8% SDS–polyacrylamide gel.

Acknowledgements

We thank B.Haarer, D.Botstein, D.Drubin, J.Pringle, F.Cross, A.Bretscher, A.Bender, M.Grunstein and A.Adams for providing plasmids and strains. We thank P.Brennwald for a generous gift of Sso1p antibody. Thanks also to the members of the Lew, Pringle and Kornbluth laboratories for stimulating discussions. This work was funded by grants from the NIH (GM53050) and the Leukemia and Lymphoma Society to D.J.L.

References

Adams,A.E.M., Botstein,D. and Drubin,D.G. (1991) Requirement of yeast fimbrin for actin organization and morphogenesis *in vivo*. *Nature*, **354**, 404–408.

Adams,A.E., Cooper,J.A. and Drubin,D.G. (1993) Unexpected combinations of null mutations in genes encoding the actin cytoskeleton are lethal in yeast. *Mol. Biol. Cell*, **4**, 459–468.

Amatruda,J.F., Cannon,J.F., Tatchell,K., Hug,C. and Cooper,J.A. (1990) Disruption of the actin cytoskeleton in yeast capping protein mutants. *Nature*, **344**, 352–354.

Amberg,D.C., Zahner,J.E., Mulholland,J.W., Pringle,J.R. and Botstein,D. (1997) Aip3p/Bud6p, a yeast actin-interacting protein that is involved in morphogenesis and the selection of bipolar budding sites. *Mol. Biol. Cell*, **8**, 729–753.

Amon,A., Surana,U., Muroff,I. and Nasmyth,K. (1992) Regulation of $p34^{CDC28}$ tyrosine phosphorylation is not required for entry into mitosis in *S.cerevisiae*. *Nature*, **355**, 368–371.

Araki,H., Leem,S.-H., Phongdara,A. and Sugino,A. (1995) Dpb11, which interacts with DNA polymerase II(e) in *Saccharomyces cerevisiae*, has a dual role in S-phase progression and at a cell cycle checkpoint. *Proc. Natl Acad. Sci. USA*, **92**, 11791–11795.

Barral,Y., Parra,M., Bidlingmaier,S. and Snyder,M. (1999) Nim1-related kinases coordinate cell cycle progression with the organization of the peripheral cytoskeleton in yeast. *Genes Dev.*, **13**, 176–187.

Barrett,T. *et al.* (1997) The structure of the GTPase-activating domain from p50rhoGAP. *Nature*, **385**, 458–461.

Baudin,A., Ozier-Kalogeropoulos,O., Denouel,A., Lacroute,F. and Cullin,C. (1993) A simple and efficient method for direct gene deletion in *Saccharomyces cerevisiae*. *Nucleic Acids Res.*, **21**, 3329–3330.

Bender,A. and Pringle,J.R. (1989) Multicopy suppression of the cdc24 budding defect in yeast by CDC42 and three newly identified genes including the ras-related gene *RSR1*. *Proc. Natl Acad. Sci. USA*, **86**, 9976–9980.

Bender,A. and Pringle,J.R. (1991) Use of a screen for synthetic lethal

and multicopy suppressee mutants to identify two new genes involved in morphogenesis in *Saccharomyces cerevisiae*. *Mol. Cell. Biol.*, **11**, 1295–1305.

Bender,L., Shuen Lo,H., Lee,H., Kokojan,V., Peterson,J. and Bender,A. (1996) Associations among PH and SH3 domain-containing proteins and Rho-type GTPases in yeast. *J. Cell Biol.*, **133**, 879–894.

Benton,B.K., Tinkelenberg,A., Gonzalez,I. and Cross,F.R. (1997) Cla4p, a *Saccharomyces cerevisiae* Cdc42p-activated kinase involved in cytokinesis, is activated at mitosis. *Mol. Cell. Biol.*, **17**, 5067–5076.

Bi,E., Chiavetta,J.B., Chen,H., Chen,G.C., Chan,C.S. and Pringle,J.R. (2000) Identification of novel, evolutionarily conserved Cdc42p-interacting proteins and of redundant pathways linking Cdc24p and Cdc42p to actin polarization in yeast. *Mol. Biol. Cell*, **11**, 773–793.

Cabib,E., Drgonova,J. and Drgon,T. (1998) Role of small G proteins in yeast cell polarization and wall biosynthesis. *Annu. Rev. Biochem.*, **67**, 307–333.

Chant,J., Corrado,K., Pringle,J.R. and Herskowitz,I. (1991) Yeast BUD5, encoding a putative GDP–GTP exchange factor, is necessary for bud site selection and interacts with bud formation gene *BEM1*. *Cell*, **65**, 1213–1224.

Chen,G.C., Zheng,L. and Chan,C.S. (1996) The LIM domain-containing Dbm1 GTPase-activating protein is required for normal cellular morphogenesis in *Saccharomyces cerevisiae*. *Mol. Cell. Biol.*, **16**, 1376–1390.

Chenevert,J., Corrado,K., Bender,A., Pringle,J. and Herskowitz,I. (1992) A yeast gene (*BEM1*) necessary for cell polarization whose product contains two SH3 domains. *Nature*, **356**, 77–79.

Chuang,T.H., Xu,X., Kaartinen,V., Heisterkamp,N., Groffen,J. and Bokoch,G.M. (1995) Abr and Bcr are multifunctional regulators of the Rho GTP-binding protein family. *Proc. Natl Acad. Sci. USA*, **92**, 10282–10286.

Cid,V.J., Cenamor,R., Sanchez,M. and Nombela,C. (1998) A mutation in the Rho1-GAP-encoding gene *BEM2* of *Saccharomyces cerevisiae* affects morphogenesis and cell wall functionality. *Microbiology*, **144**, 25–36.

Cid,V.J., Adamikova,L., Sanchez,M., Molina,M. and Nombela,C. (2001) Cell cycle control of septin ring dynamics in the budding yeast. *Microbiology*, **147**, 1437–1450.

Coleman,T.R. and Dunphy,W.G. (1994) Cdc2 regulatory factors. *Curr. Opin. Cell Biol.*, **6**, 877–882.

Coleman,T.R., Tang,Z. and Dunphy,W.G. (1993) Negative regulation of the Wee1 protein kinase by direct action of the nim1/cdr1 mitotic inducer. *Cell*, **72**, 919–929.

Furnari,B., Rhind,N. and Russell,P. (1997) Cdc25 mitotic inducer targeted by Chk1 DNA damage checkpoint kinase. *Science*, **277**, 1495–1497.

Furukawa,Y., Kawasoe,T., Daigo,Y., Nishiwaki,T., Ishiguro,H., Takahashi,M., Kitayama,J. and Nakamura,Y. (2001) Isolation of a novel human gene, *ARHGAP9*, encoding a rho-GTPase activating protein. *Biochem. Biophys. Res. Commun.*, **284**, 643–649.

Gardner,R.D., Poddar,A., Yellman,C., Tavormina,P.A., Monteagudo, M.C. and Burke,D.J. (2001) The spindle checkpoint of the yeast *Saccharomyces cerevisiae* requires kinetochore function and maps to the CBF3 domain. *Genetics*, **157**, 1493–1502.

Gehrung,S. and Snyder,M. (1990) The SPA2 gene of *Saccharomyces cerevisiae* is important for pheromone-induced morphogenesis and efficient mating. *J. Cell Biol.*, **111**, 1451–1464.

Gladfelter,A.S., Bose,I., Zyla,T.R., Bardes,E.S. and Lew,D.J. (2002) Septin ring assembly involves cycles of GTP loading and hydrolysis by Cdc42p. *J. Cell Biol.*, **156**, 315–326.

Guthrie,C. and Fink,G.R. (eds) (1991) Guide to yeast genetics and molecular biology. *Methods Enzymol.*, **194**, 933.

Haarer,B.K., Petzold,A.S. and Brown,S.S. (1993) Mutational analysis of yeast profilin. *Mol. Cell. Biol.*, **13**, 7864–7873.

Harrison,J.C., Bardes,E.S., Ohya,Y. and Lew,D.J. (2001) A role for the Pkc1p/Mpk1p kinase cascade in the morphogenesis checkpoint. *Nat. Cell Biol.*, **3**, 417–420.

Kamada,Y., Jung,U.S., Piotrowski,J. and Levin,D.E. (1995) The protein kinase C-activated MAP kinase pathway of *Saccharomyces cerevisiae* mediates a novel aspect of the heat shock response. *Genes Dev.*, **9**, 1559–1571.

Kim,Y.J., Francisco,L., Chen,G.C., Marcotte,E. and Chan,C.S. (1994) Control of cellular morphogenesis by the Ip12/Bem2 GTPase-activating protein: possible role of protein phosphorylation. *J. Cell Biol.*, **127**, 1381–1394.

Krugmann,S. *et al.* (2002) Identification of ARAP3, a novel PI3K effector regulating both Arf and Rho GTPases, by selective capture on phosphoinositide affinity matrices. *Mol. Cell*, **9**, 95–108.

Kumagai,A. and Dunphy,W.G. (1992) Regulation of the cdc25 protein during the cell cycle in *Xenopus* extracts. *Cell*, **70**, 139–151.

Lappalainen,P., Fedorov,E.V., Fedorov,A.A., Almo,S.C. and Drubin,D.G. (1997) Essential functions and actin-binding surfaces of yeast cofilin revealed by systematic mutagenesis. *EMBO J.*, **16**, 5520–5530.

Leberer,E., Dignard,D., Harcus,D., Thomas,D.Y. and Whiteway,M. (1992) The protein kinase homologue Ste20p is required to link the yeast pheromone response G-protein bg subunits to downstream signaling components. *EMBO J.*, **11**, 4815–4824.

Lee,J., Kumagai,A. and Dunphy,W.G. (2001) Positive regulation of Wee1 by Chk1 and 14-3-3 proteins. *Mol. Biol. Cell*, **12**, 551–563.

Lehman,K., Rossi,G., Adamo,J.E. and Brennwald,P. (1999) Yeast homologues of tomosyn and lethal giant larvae function in exocytosis and are associated with the plasma membrane SNARE, Sec9. *J. Cell Biol.*, **146**, 125–140.

Lew,D.J. and Reed,S.I. (1995) A cell cycle checkpoint monitors cell morphogenesis in budding yeast. *J. Cell Biol.*, **129**, 739–749.

Li,R., Zhang,B. and Zheng,Y. (1997) Structural determinants required for the interaction between Rho GTPase and the GTPase-activating domain of p190. *J. Biol. Chem.*, **272**, 32830–32835.

Liu,H. and Bretscher,A. (1989) Disruption of the single tropomyosin gene in yeast results in the disappearance of actin cables from the cytoskeleton. *Cell*, **57**, 233–242.

Liu,Q., Li,M.Z., Leibham,D., Cortez,D. and Elledge,S.J. (1998) The univector plasmid-fusion system, a method for rapid construction of recombinant DNA without restriction enzymes. *Curr. Biol.*, **8**, 1300–1309.

Longtine,M.S., Theesfeld,C.L., McMillan,J.N., Weaver,E., Pringle,J.R. and Lew,D.J. (2000) Septin-dependent assembly of a cell cycle-regulatory module in *Saccharomyces cerevisiae*. *Mol. Cell. Biol.*, **20**, 4049–4061.

Ma,X.-J., Lu,Q. and Grunstein,M. (1996) A search for proteins that interact genetically with histone H3 and H4 amino termini uncovers novel regulators of the Swe1 kinase in *Saccharomyces cerevisiae*. *Genes Dev.*, **10**, 1327–1340.

McMillan,J.N., Sia,R.A.L. and Lew,D.J. (1998) A morphogenesis checkpoint monitors the actin cytoskeleton in yeast. *J. Cell Biol.*, **142**, 1487–1499.

McMillan,J.N., Longtine,M.S., Sia,R.A., Theesfeld,C.L., Bardes,E.S., Pringle,J.R. and Lew,D.J. (1999) The morphogenesis checkpoint in *Saccharomyces cerevisiae*: cell cycle control of Swe1p degradation by Hsl1p and Hsl7p. *Mol. Cell. Biol.*, **19**, 6929–6939.

Miura,K., Jacques,K.M., Stauffer,S., Kubosaki,A., Zhu,K., Hirsch,D.S., Resau,J., Zheng,Y. and Randazzo,P.A. (2002) ARAP1: a point of convergence for Arf and Rho signaling. *Mol. Cell.*, **9**, 109–119.

Mueller,P.R., Coleman,T.R. and Dunphy,W.G. (1995) Cell cycle regulation of a *Xenopus* Wee1-like kinase. *Mol. Biol. Cell*, **6**, 119–134.

Musacchio,A., Cantley,L.C. and Harrison,S.C. (1996) Crystal structure of the breakpoint cluster region-homology domain from phosphoinositide 3-kinase p85 α subunit. *Proc. Natl Acad. Sci. USA*, **93**, 14373–14378.

Navas,T.A., Zhou,Z. and Elledge,S.J. (1995) DNA polymerase ε links the DNA replication machinery to the S phase checkpoint. *Cell*, **80**, 29–39.

O'Farrell,P.H. (2001) Triggering the all-or-nothing switch into mitosis. *Trends Cell Biol.*, **11**, 512–519.

Oehlen,L.J. and Cross,F.R. (1998) Potential regulation of Ste20 function by the Cln1–Cdc28 and Cln2–Cdc28 cyclin-dependent protein kinases. *J. Biol. Chem.*, **273**, 25089–25097.

Parker,L.L., Walter,S.A., Young,P.G. and Piwnica-Worms,H. (1993) Phosphorylation and inactivation of the mitotic inhibitor Wee1 by the *nim1/cdr1* kinase. *Nature*, **363**, 736–738.

Peterson,J., Zheng,Y., Bender,L., Myers,A., Cerione,R. and Bender,A. (1994) Interactions between the bud emergence proteins Bem1p and Bem2p and Rho-type GTPases in yeast. *J. Cell Biol.*, **127**, 1395–1406.

Piatti,S., Lengauer,C. and Nasmyth,K. (1995) Cdc6 is an unstable protein whose *de novo* synthesis in G_1 is important for the onset of S phase and for preventing a 'reductional' anaphase in the budding yeast *Saccharomyces cerevisiae*. *EMBO J.*, **14**, 3788–3799.

Pringle,J.R., Bi,E., Harkins,H.A., Zahner,J.E., De Virgilio,C., Chant,J., Corrado,K. and Fares,H. (1995) Establishment of cell polarity in yeast. *Cold Spring Harb. Symp. Quant. Biol.*, **60**, 729–744.

Pruyne,D. and Bretscher,A. (2000a) Polarization of cell growth in yeast. *J. Cell Sci.*, **113**, 571–585.

Pruyne,D. and Bretscher,A. (2000b) Polarization of cell growth in yeast. *J. Cell Sci.*, **113**, 365–375.

Ridley,A.J. (1995) Rho-related proteins: actin cytoskeleton and cell cycle. *Curr. Opin. Genet. Dev.*, **5**, 24–30.

Sia,R.A.L., Herald,H.A. and Lew,D.J. (1996) Cdc28 tyrosine phosphorylation and the morphogenesis checkpoint in budding yeast. *Mol. Biol. Cell*, **7**, 1657–1666.

Sia,R.A.L., Bardes,E.S.G. and Lew,D.J. (1998) Control of Swe1p degradation by the morphogenesis checkpoint. *EMBO J.*, **17**, 6678–6688.

Sikorski,R.S. and Hieter,P. (1989) A system of shuttle vectors and yeast host strains designed for efficient manipulation of DNA in *Saccharomyces cerevisiae*. *Genetics*, **122**, 19–27.

Sorger,P.K. and Murray,A.W. (1992) S-phase feedback control in budding yeast independent of tyrosine phosphorylation of $p34^{CDC28}$. *Nature*, **355**, 365–368.

Stueland,C.S., Lew,D.J., Cismowski,M.J. and Reed,S.I. (1993) Full activation of $p34^{CDC28}$ histone H1 kinase activity is unable to promote entry into mitosis in checkpoint-arrested cells of the yeast *Saccharomyces cerevisiae*. *Mol. Cell. Biol.*, **13**, 3744–3755.

Sugimoto,K., Shimomura,T., Hashimoto,K., Araki,H., Sugino,A. and Matsumoto,K. (1996) Rfc5, a small subunit of replication factor C complex, couples DNA replication and mitosis in budding yeast. *Proc. Natl Acad. Sci. USA*, **93**, 7048–7052.

Tong,A.H. *et al.* (2001) Systematic genetic analysis with ordered arrays of yeast deletion mutants. *Science*, **294**, 2364–2368.

Wang,T. and Bretscher,A. (1995) The rho-GAP encoded by BEM2 regulates cytoskeletal structure in budding yeast. *Mol. Biol. Cell*, **6**, 1011–1024.

Watanabe,D., Abe,M. and Ohya,Y. (2001) Yeast Lrg1p acts as a specialized RhoGAP regulating 1,3-β-glucan synthesis. *Yeast*, **18**, 943–951.

Wertman,K.F., Drubin,D.G. and Botstein,D. (1992) Systematic mutational analysis of the yeast *ACT1* gene. *Genetics*, **132**, 337–350.

Wirth,J.A., Jensen,K.A., Post,P.L., Bement,W.M. and Mooseker,M.S. (1996) Human myosin-IXb, an unconventional myosin with a chimerin-like rho/rac GTPase-activating protein domain in its tail. *J. Cell Sci.*, **109**, 653–661.

Wu,L. and Russell,P. (1993) Nim1 kinase promotes mitosis by inactivating Wee1 tyrosine kinase. *Nature*, **363**, 738–741.

Yamamoto,A., Guacci,V. and Koshland,D. (1996) Pds1p, an inhibitor of anaphase in budding yeast, plays a critical role in the APC and checkpoint pathway(s). *J. Cell Biol.*, **133**, 99–110.

Yeh,J. and Haarer,B.K. (1996) Profilin is required for the normal timing of actin polymerization in response to thermal stress. *FEBS Lett.*, **398**, 303–307.

Zahner,J.E., Harkins,H.A. and Pringle,J.R. (1996) Genetic analysis of the bipolar pattern of bud site selection in the yeast *Saccharomyces cerevisiae*. *Mol. Cell. Biol.*, **16**, 1857–1870.

Received April 3, 2002; revised and accepted June 17, 2002